ADVANCED PHYSICS RESEARCH Open Access
www.advphysicsres.com

High-Throughput Optimization of Magnetoresistance Materials Based on Lock-In Thermography

Rajkumar Modak, Takamasa Hirai, Yuya Sakuraba, Seiji Mitani, Koichi Oyanagi, Takumi Yamazaki, Takeshi Seki, and Ken-ichi Uchida**

With the giant magnetoresistance (GMR) effect serving as a vital component in modern spintronic technologies, researchers are dedicating significant efforts to improve the performance of GMR devices through material exploration and design optimization. However, traditional GMR measurement approaches are inefficient for comprehensive material and device optimization. This study proposes a high-throughput current-in-plane GMR measurement technique based on thermal imaging of Joule heating utilizing lock-in thermography (LIT). This LIT-based technique is advantageous for efficiently evaluating films with varying compositions and thickness gradients, which is crucial for ongoing material exploration and design optimization to enhance the GMR ratio. First, it is demonstrated that using CoFe/Cu multilayers, the simple Joule heating measurement based on LIT enables quantitative estimation of the GMR ratio. Then, to confirm the usefulness of the proposed method in high-throughput material screening, a case study is shown to investigate the GMR of CoCu-based granular films with a composition gradient. These techniques allow to determine the optimum composition with maximum GMR ratio using the single composition-gradient film and reveal $Co_{22}Cu_{78}$ as the optimal composition, yielding the largest GMR ratio among the reported polycrystalline CoCu-based granular films. This demonstration accelerates the material and structural optimization of GMR devices.

1. Introduction

The giant magnetoresistance (GMR) effect, discovered in Fe/Cr superlattices in 1988,[1,2] is a phenomenon where the resistance of a metallic multilayer, consisting of ferromagnetic (FM) and nonmagnetic (NM) layers, changes depending on the magnetization direction of each FM layer. Later, GMR was found also in several bi-metallic or multi-metallic layers containing FM and antiferromagnetic or NM metals, as well as single-layer granular materials.[3–7] Since its discovery, GMR has been the subject of extensive research to understand the underlying physics and exploit its vast technical applications. Over past decades, the applications of GMR concepts have extended across diverse domains, from revolutionizing read/write heads in hard disk drives[8] to automotive sensors,[9] biomedical sensors,[10] flexible strain sensors,[11] non-destructive materials testing,[12] and beyond.

In recent years, current-in-plane (CIP) GMR devices have attracted renewed interest due to their structural simplicity and ease of fabrication, making them promising candidates for high-sensitivity magnetic field sensors,[13,14] biosensors,[15,16] emerging spin-orbit torque devices,[17] and flexible electronics.[18,19] However, the CIP-GMR ratios in conventional materials are often lower compared to tunneling magnetoresistance[20–24] and current-perpendicular-to-plane GMR,[25–28] limiting their sensitivity in these emerging applications. Therefore, research is ongoing to optimize material and device design for improved CIP-GMR performance. Researchers actively explore material

R. Modak, T. Hirai, Y. Sakuraba, S. Mitani, K. Oyanagi, T. Seki, K. Uchida
National Institute for Materials Science
Tsukuba 305-0047, Japan
E-mail: modak.rajkumar@nims.go.jp; uchida.kenichi@nims.go.jp

The ORCID identification number(s) for the author(s) of this article can be found under https://doi.org/10.1002/apxr.202400021

DOI: 10.1002/apxr.202400021

K. Oyanagi
Faculty of Science and Engineering
Iwate University
Morioka 020-8551, Japan

T. Yamazaki, T. Seki, K. Uchida
Institute for Materials Research
Tohoku University
Sendai 980-8577, Japan

T. Seki
Center for Science and Innovation in Spintronics
Tohoku University
Sendai 980-8577, Japan

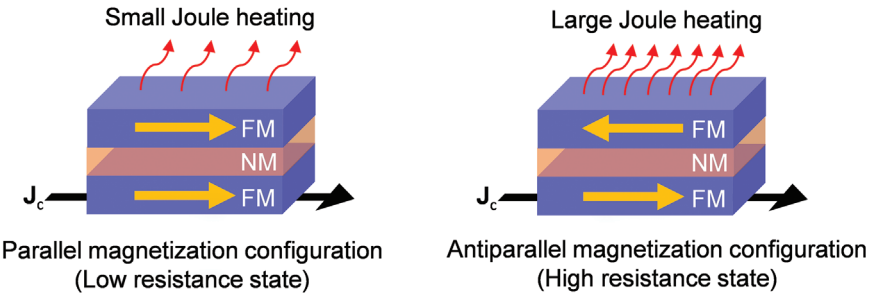

Figure 1. Joule heating in materials with GMR. Schematic of the change in Joule heating due to current-in-plane GMR in a ferromagnetic metal (FM)/nonmagnetic metal (NM) multilayer. With a parallel (antiparallel) magnetization configuration of the FM layers, the multilayer has a low (high) electrical resistance, which results in small (large) Joule heating when a charge current $\mathbf{J}_c$ is passed. The same situation occurs in a magnetic granular material when it exhibits GMR.

compositions, layer structures, and fabrication techniques, seeking higher GMR ratios and improved stability. Various approaches have been adopted for this purpose. The systematic tuning of FM layer composition and thickness,[29–31] NM spacer layer thickness,[3,32] and seed layer composition and thickness[33–35] are a few popular methods for improving the GMR response.

Despite these efforts, the complexity and time-consuming nature of systematic GMR measurements for uniform films with various compositions/thicknesses remain significant barriers to high-throughput material screening, which is crucial for effectively identifying promising materials with desirable GMR properties. In recent years, researchers have used wedge-shaped films to determine the optimal thickness for spacer layers effectively.[36,37] However, this method requires the formation of microstructured devices and subsequent GMR measurements in each device. The limited number of devices achievable along the composition gradient during microfabrication restricts the minimum difference in composition that can be investigated. This, coupled with the time-consuming process of measuring GMR for each device individually, significantly limits the utility of this approach for high-throughput material screening. Also, the discrete data points from individual microfabricated devices may result in overlooking the optimum condition for the best GMR ratio. Therefore, it is necessary to develop an alternative measurement approach that overcomes these limitations and expedites the screening and optimization of GMR materials.

This study addresses this need by introducing and validating a simple and effective CIP-GMR measurement method based on thermal imaging of Joule heating, utilizing the lock-in thermography (LIT) technique.[38–41] The resistance R of a material exhibiting the GMR effect experiences significant variations concurrent with the changes in its magnetization configuration due to the influence of the external magnetic field H. The GMR ratio is determined as $\Delta R/R$, where ΔR is the change in resistance between parallel and antiparallel magnetization states (between high-H and zero-H conditions) in multilayer (granular) film. When a charge current J_c is applied to the material to measure the GMR effect, Joule heating Q also appears, where $Q \propto J_c^2 R$. Given the direct proportionality between Joule heating and R, the relationship to quantify GMR can also be expressed as $\Delta Q/Q$, where ΔQ is the change in the heat release due to Joule heating between parallel and antiparallel magnetization state (between high-H and zero-H conditions) in a multilayer (granular) film (**Figure 1**), suggesting a possibility of quantifying the GMR ratio through the Joule-heating measurement.

Building upon this foundational understanding, we employed the LIT technique to measure the temperature modulation induced by Joule heating in a conductor for GMR estimation. The LIT method allows for highly sensitive Joule-heating measurements and also suppression of parasitic effects due to thermal diffusion by measuring the temperature modulation at a high lock-in frequency.[39,40] This study shows the precise estimation of the CIP-GMR ratio from thermal images of Joule heating for a CoFe/Cu multilayer film, demonstrating the accuracy of this method. Then, a comprehensive case study on CoCu-based granular films is presented. This study showcases the ability of the proposed techniques to simultaneously estimate composition-dependent GMR, thereby highlighting its utility for high-throughput GMR material investigation. The experiments also unveil the optimal composition of the granular film to be $Co_{22}Cu_{78}$, achieving a large room-temperature GMR ratio exceeding 8% at $\mu_0 H = 0.9$ T, where μ_0 denotes the vacuum permeability, and a saturation GMR ratio of ≈28% at 4 K, record-high values for polycrystalline CoCu-based single-layer granular materials.[42–45] These results emphasize the accuracy and versatility of the LIT-based method and demonstrate its potential to drive advancements in material exploration and device optimization in spintronics.

2. Results and Discussion

2.1. Validation of LIT-Based GMR Measurement Method

To validate the reliability of the proposed LIT-based GMR measurement method, we conducted experiments using a uniform reference material: the epitaxial CoFe/Cu multilayer film. This film is known to exhibit a very large CIP-GMR ratio at room temperature.[36,46] The film was structured into a strip geometry with a width of 0.2 mm and a length of 6.0 mm for the measurement. The temperature modulation due to Joule heating was recorded using the LIT technique while an ON/OFF-modulated AC charge current with an ON-state current magnitude of J_c and frequency f was applied to the sample along the length direction. The experimental configuration for the LIT measurements is shown in **Figure 2a**. Using an infrared camera, we recorded thermal images of the surface of the CoFe/Cu multilayer film and

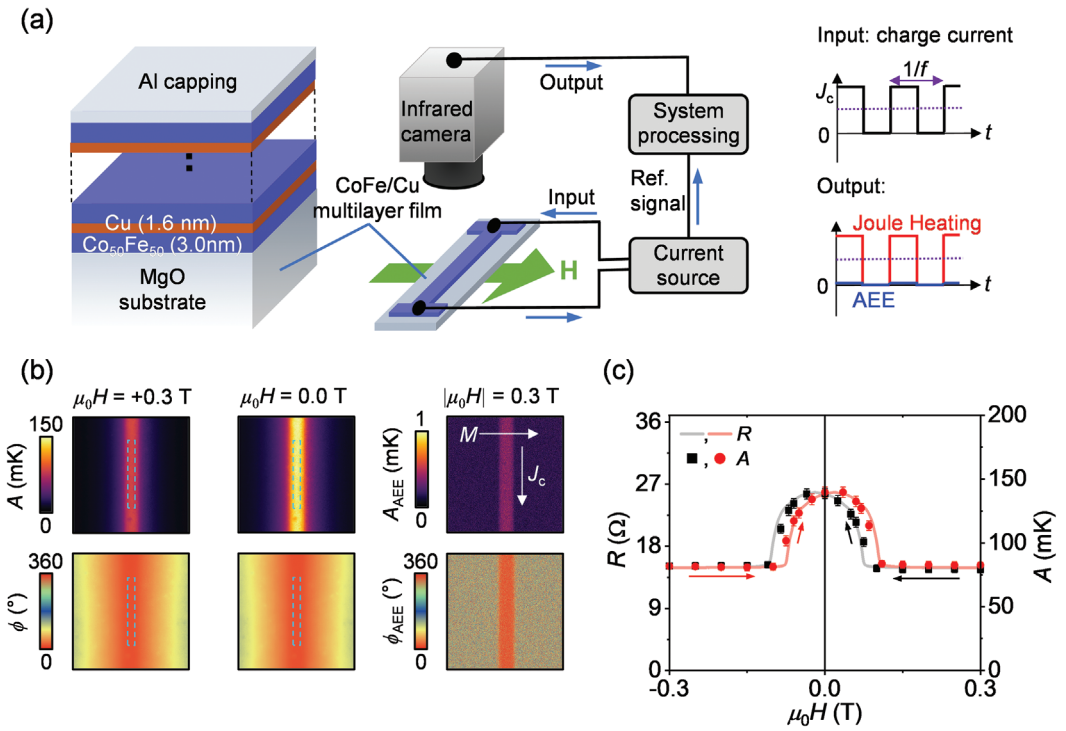

Figure 2. Thermal imaging of Joule heating using LIT. a) Schematics of the CoFe/Cu multilayer film structure used in the present study and the experimental setup for measuring the change in Joule-heating-induced temperature modulation due to GMR when J_c is applied to the film. During the LIT measurements, an ON/OFF-modulated AC charge current with an ON-state current magnitude J_c and frequency f was applied to the sample. Under these conditions, the output Joule heating oscillates with the same f as the applied current, as illustrated in the input and output time charts. b) Lock-in amplitude (A) and phase (ϕ) signals produced by Joule heating in the CoFe/Cu multilayer film, acquired at J_c = 60 mA and f = 25.0 Hz, and applied magnetic fields of $\mu_0 H = +0.3$ and 0.0 T. μ_0 denotes the vacuum permeability. A_{AEE} and ϕ_{AEE} represent the signals produced by the anomalous Ettingshausen effect (AEE) for the film at $|\mu_0 H| = 0.3$ T. During the AEE measurement, J_c = 60 mA, f = 25 Hz, and zero DC offset was applied to the sample.[48–52] c) H dependence of the A signal obtained from the Joule heating measurements on the CoFe/Cu multilayer film, recorded at discrete magnetic field values during the incremental and decremental sweeps of H. The A values were obtained by averaging the raw signals in an area of 0.1 × 0.9 mm^2 on the sample, as represented by the dashed rectangular box in b). The error bars represent the standard deviations of the data in the corresponding rectangular box. The solid curves represent the H dependence of the electrical resistance R of the film measured by the four-probe method by applying a 60 mA direct current.

extracted the charge-current-induced temperature change oscillating at the same f as the J_c through Fourier analysis. The obtained thermal images were transformed into lock-in amplitude A and phase ϕ images, where A represents the magnitude of the charge-current-induced temperature change and ϕ indicate the sign and time delay of the temperature change. We coated the sample surface with a thin layer of insulating black ink. This ink has a very high infrared emissivity of > 0.94, guaranteeing a strong and consistent infrared emission signal regardless of the inherent emissivity of the material and improving the signal-to-noise ratio in the measured data. Consequently, the black ink coating in this measurement broadens the scope of materials that can be studied. All measurements were performed at room temperature and atmospheric pressure.

To evaluate the GMR-induced change in Joule heating, we recorded the $\mu_0 H$ dependence of A and ϕ images of the CoFe/Cu multilayer film at J_c = 60 mA and f = 25.0 Hz, with H applied along the width direction. The measurements were performed at the maximum available lock-in frequency of the system to disregard the effects of heat convection on the environment.[47] Figure 2b displays the representative A and ϕ images recorded at $\mu_0 H = +0.3$ and 0.0 T. It is important to note that the LIT images obtained at a finite H may encompass signals arising from the anomalous Ettingshausen effect (AEE).[48–52] However, for the present CoFe/Cu multilayer film, the AEE signals are smaller than the noise level of the Joule-heating contribution (Figure 2b). This implies that the observed LIT images predominantly reflect Joule heating effects, allowing us to disregard AEE contribution in A for our GMR estimation. The $\mu_0 H$ dependence of A, obtained by averaging the region indicated by the dashed rectangular box in Figure 2b covering an area of 0.1 × 0.9 mm^2, is presented in Figure 2c as discrete data points. In this figure, we compare the $\mu_0 H$ dependence of A with that of R of the sample, represented by solid lines. The $\mu_0 H$ dependence of R was measured by continuously sweeping $\mu_0 H$ from +0.3 to −0.3 T in forward and reverse directions and recording R using the conventional four-probe method. The results indicate that the magnitude of A follows the same H dependence as R, suggesting that the relative variations in R can be determined from the LIT images, providing a means of calculating the GMR ratio based on the relation $\Delta Q/Q = \Delta R/R$. For the LIT images of the present CoFe/Cu multilayer film, $\Delta Q/Q$ can be rewritten as $\Delta A/A = (A_H - A_0)/A_0$. Here, A_H (A_0) represents the Joule-heating-induced A signal at the parallel (antiparallel) magnetization state at high (zero) H.[36]

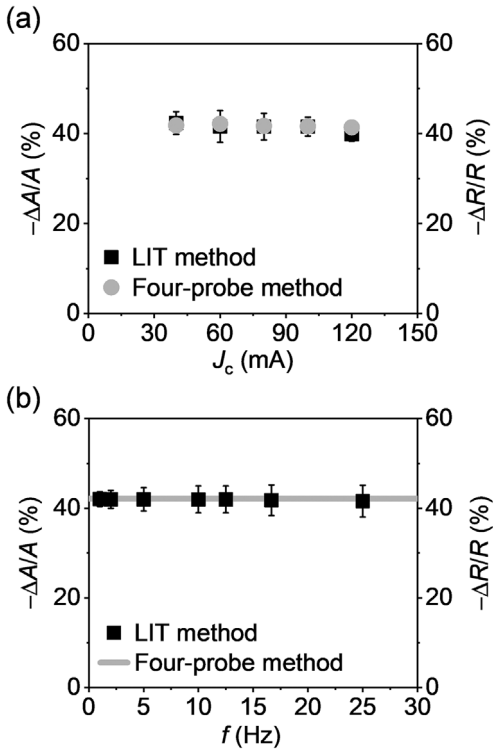

Figure 3. Estimation of GMR ratio from thermal imaging of Joule heating. a) J_c dependence of the magnetic-field-induced change ratio of the Joule heating amplitude $\Delta A/A = (A_{+0.3\,T} - A_{0.0\,T})/A_{0.0\,T}$ (black squares) acquired at $f = 25.0$ Hz. Here, $A_{+0.3\,T}$ and $A_{0.0\,T}$ represent the A values at $\mu_0 H = +0.3$ and 0.0 T, respectively. Gray circles represent the GMR ratio $\Delta R/R = (R_{+0.3\,T} - R_{0.0\,T})/R_{0.0\,T}$, where $R_{+0.3\,T}$ and $R_{0.0\,T}$ are the resistances of the film at $\mu_0 H = +0.3$ and 0.0 T, respectively, estimated by the conventional four-probe method. b) f dependence of $\Delta A/A$, acquired at $J_c = 60$ mA. The gray line represents the $\Delta R/R$ value estimated by the conventional four-probe method.

It is noteworthy that if the AEE contribution is substantial and the samples exhibit small or no hysteresis, the AEE contribution can be eliminated for the GMR estimation by calculating the H-even-dependent component of A (i.e., A_{even}) using LIT images recorded at $\pm H$ and replacing A_H with A_{even} because the AEE signal exhibits the H-odd dependence.[48–52] However, for the present CoFe/Cu multilayer film with tiny AEE and substantial hysteresis, we focus on raw LIT images.

Now, we present the quantitative determination of the CIP-GMR ratio for the CoFe/Cu multilayer film utilizing the LIT images. **Figure 3a** represents $\Delta A/A = (A_{+0.3\,T} - A_{0.0\,T})/A_{0.0\,T}$ as a function of J_c with discrete black squares. Here, $A_{+0.3\,T}$ and $A_{0.0\,T}$ denote the averaged A values acquired at $\mu_0 H = +0.3$ and 0.0 T, respectively. The data show the J_c independence of $\Delta A/A$, which is consistent with the nature of GMR. To compare $\Delta A/A$ with the conventional GMR ratio $\Delta R/R$ of the film, we further assessed the J_c-dependent $\Delta R/R$ through conventional four-probe GMR measurements, as represented by gray circles in Figure 3a. Additionally, we compared $\Delta A/A$ obtained using f-dependent LIT measurements with $\Delta R/R$ obtained using the four-probe method in Figure 3b. The results confirm that the $\Delta A/A$ values estimated using the LIT technique agree with the GMR ratio $\Delta R/R$ obtained via the conventional four-probe measurements, thereby validating the proposed LIT-based GMR measurement method. These findings confirm that the GMR ratio can be accurately estimated using the LIT-based thermal images of Joule heating. It is important to note that the observed A due to Joule heating strongly depends on the thermal conductivity of the substrate through heat conduction. As the thermal conductivity increases, heat transfer from the film to the substrate increases, leading to a decrease in measured A.[39,51] However, because the rate of heat transfer to the substrate is independent of the positions, the relative change of the A signal at each H is not affected by the substrate species. Thus, the GMR can be estimated from the Joule heating images regardless of the substrate choice. Nevertheless, films on substrates with lower thermal conductivities will provide larger A signals, resulting in a better signal-to-noise ratio compared to those on substrates with high thermal conductivities substrate for the same charge current value.

2.2. Demonstration of High-Throughput Magnetoresistance Material Screening

To demonstrate the utility of the proposed LIT-based GMR measurement method for high-throughput material screening, we present a case study involving CoCu-based granular single-layer films. The observation of the GMR effect using the LIT method is possible not only for the FM/NM multilayers but also for various phase-separated granular films (e.g., Co–Cu, Co–Ag).[5,6,53,54] The GMR properties of $Co_{100-q}Cu_q$ granular films have been extensively investigated across various composition regions by diverse research groups over several decades.[5,6,42–44,54–56] Within the scope of these studies, the composition range of $70 \leq q \leq 90$ at.% is expected to exhibit large GMR ratios. However, existing studies have primarily focused on selecting film compositions, resulting in a lack of systematic information for compositional variations. The present study addresses this research gap by utilizing the proposed technique to systematically explore the composition-dependent GMR behavior of the $Co_{100-q}Cu_q$ granular films.

Employing a combinatorial deposition technique,[57–59] we fabricated two 100 nm-thick $Co_{100-q}Cu_q$ films with varying compositions from $q = 65.0$ to 100.0 at.% on single quartz glass substrates at room temperature. One of the films was used in the as-deposited state, while the other film was annealed at 573 K for 10 min after the deposition to boost the formation of the granular structure. These films have linear composition gradients spanning a length of 7.0 mm on a single substrate of a 10.0×10.0 mm^2 dimension (**Figure 4a**). The distribution of the film composition was confirmed by position-dependent composition measurements using an electron probe microanalyzer with a spot size of 5 μm in diameter, as shown in Figure 4b. Figure 4c,d shows the 2D image profiles of out-of-plane X-ray diffraction (XRD) measurements for the as-deposited and 573 K-annealed $Co_{100-q}Cu_q$ composition-gradient films, respectively, measured at different positions along the composition gradient. In all composition regions for both films, the 2D XRD scans revealed an fcc diffraction pattern, similar to that of a pure Cu film, indicating that the Co is dispersed in the fcc-Cu matrix. However, as the Co concentration increased, the diffraction peak position

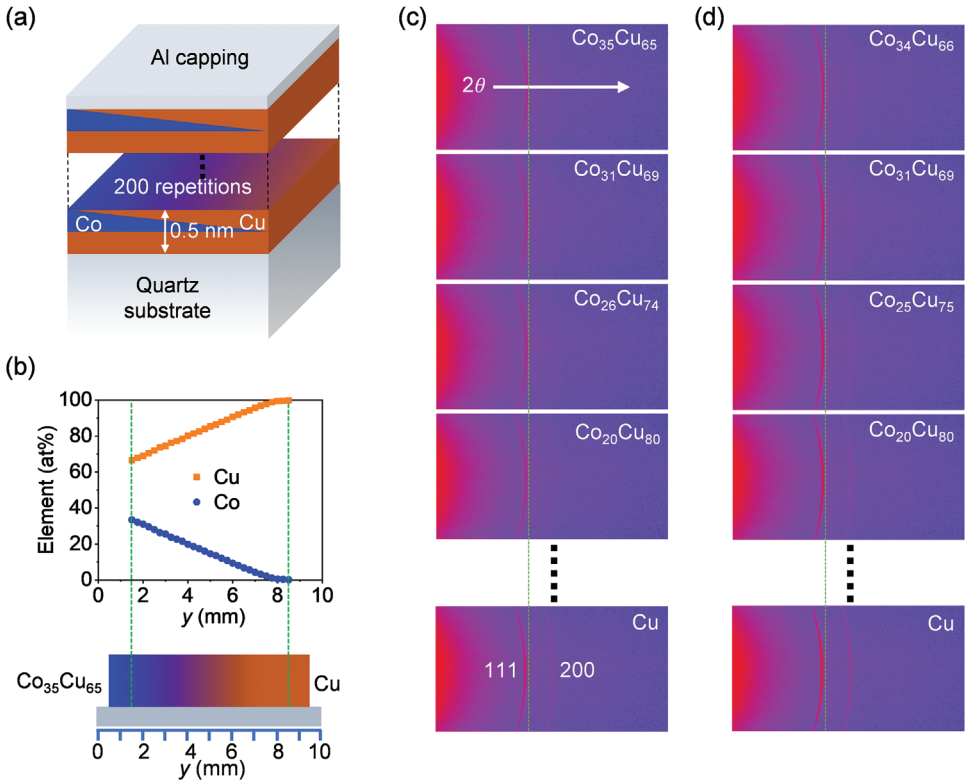

Figure 4. Fabrication of CoCu-based composition-gradient granular films. a) Schematic of the $Co_{100-q}Cu_q$ composition-gradient film structure, where a uniform Cu layer and wedge-shaped Co and Cu layers were alternately deposited on a quartz glass substrate using a linear moving shutter and a sample holder rotator. b) Position *y* dependence of the film composition measured by thermal emission electron probe microanalyzer. c,d) 2D XRD profiles for the as-deposited c) and 573 K-annealed d) $Co_{100-q}Cu_q$ composition-gradient films measured at 1 mm intervals along the composition gradient. The compositions written on the 2D profile were estimated from the *y*-dependent composition data.

shifted to a higher angle of 2θ due to a decrease in lattice parameters. The ring-shaped diffraction pattern observed in the 2D images indicates the polycrystalline nature of the films.

We estimated the composition dependence of GMR for the as-deposited and 573 K-annealed $Co_{100-q}Cu_q$ films utilizing LIT images. We fabricated wire-shaped structures from both films having a width of 1.0 mm and a length of 8.0 mm, with the composition gradient along the length direction. During the LIT measurements, the wires from the as-deposited and 573 K-annealed films were electrically connected, forming a U-shaped configuration with charge currents flowing in opposite directions along the length (composition gradient) direction, as illustrated in **Figure 5**a. For the GMR estimation, we collected *A* and ϕ images induced by an ON/OFF-modulated charge current with $J_c = 60$ mA and $f = 25.0$ Hz at $\mu_0 H = +0.9$ and 0.0 T. It should be noted that the LIT measurements at a high lock-in frequency are important to suppress the effect of thermal diffusion for composition-gradient film.[39,40] *H* was applied in a direction perpendicular to the composition gradient. Following the previously described procedure, we extracted $\Delta A\ (= A_{+0.9\,T} - A_{0.0\,T})$ utilizing the *A* images acquired at $\mu_0 H = +0.9$ and 0.0 T, as shown in Figure 5b. Here, we neglect the AEE contribution to the measured *A* images at $\mu_0 H = +0.9$ T due to its negligibly small value as compared to the Joule heating contribution. Subsequently, we estimated composition-dependent $\Delta A/A$, utilizing the line profiles for the ΔA image and the *A* image at $\mu_0 H = 0.0$ T obtained by averaging data points over 0.6 mm along the width direction represented by the white dashed region in Figure 5b. Figure 5c shows the *q* dependence of $\Delta A/A$ for the as-deposited and 573 K-annealed $Co_{100-q}Cu_q$ films. The data reveal that the $\Delta A/A$, representing the GMR ratio for the film, gradually increases beyond $q > 65$ at.%, reaching a peak near $q = 78$ at.% for the 573 K-annealed film and $q = 80$ at.% for the as-deposited film, and then gradually decreases to zero for pure Cu ($q = 100$ at.%). This observed trend in the *q*-dependence of the GMR ratio for the $Co_{100-q}Cu_q$ films aligns well with previous findings reported in the literature.[42] The outcomes distinctly identify the optimal compositions for large room-temperature GMR for both films simultaneously, all obtained through the single LIT measurement. Additionally, the composition resolution achieved with the LIT-based GMR measurement is significantly higher compared to conventional GMR measurement methods. For instance, each data point in Figure 5c (corresponding to a pixel in the LIT image of Figure 5b) represents a composition change of ≈0.075 at.%, which can be further improved by decreasing the composition gradient. Although the actual special resolution is worse than the pixel size due to the temperature broadening in the black ink layer, the composition resolution is still sufficiently excellent to accelerate the GMR studies. Interestingly, the data in Figure 5c reveal that the optimal compositions for maximum GMR at room temperature differ between as-deposited and 573 K-annealed $Co_{100-q}Cu_q$ films. This difference can be attributed to the formation of Co precip-

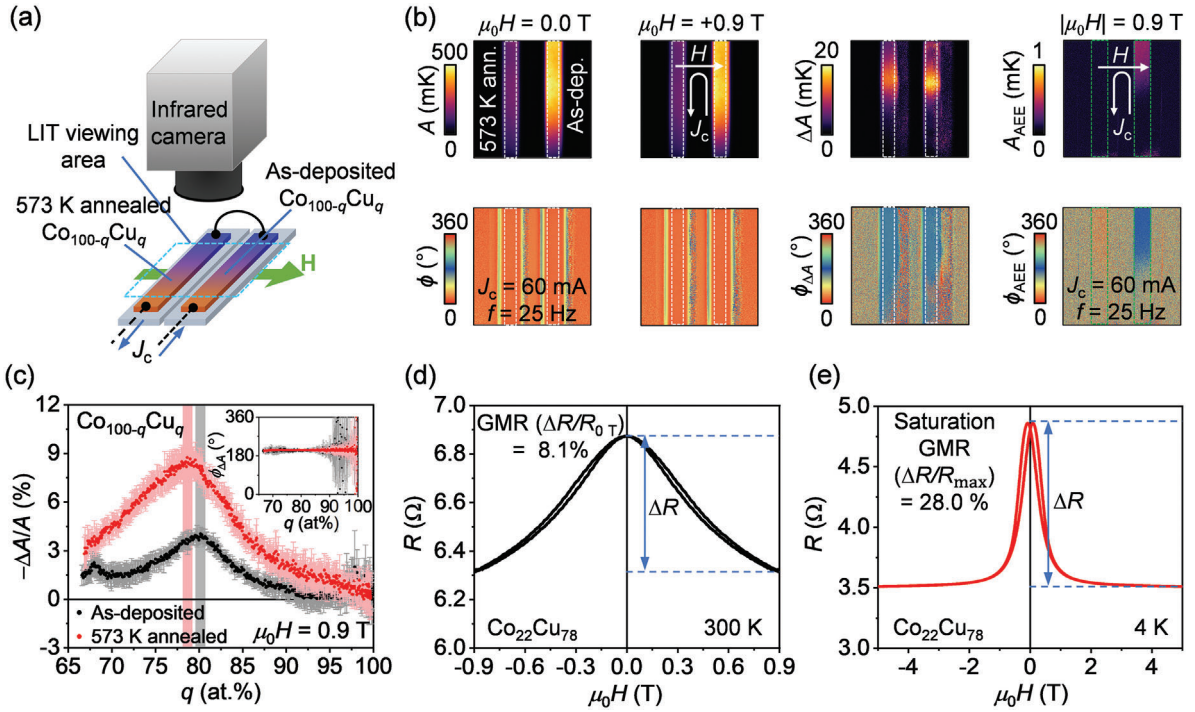

Figure 5. LIT-based high-throughput measurement of composition-dependent GMR for CoCu-based granular films. a) Schematic of the experimental setup designed for the concurrent measurement of GMR in the as-deposited and 573 K-annealed $Co_{100-q}Cu_q$ composition-gradient films. b) A, ϕ, ΔA, and $\phi_{\Delta A}$ images resulting from Joule heating of the films, acquired at J_c = 60 mA, f = 25.0 Hz, and μ_0H of +0.9 and 0.0 T and A_{AEE} and ϕ_{AEE} images resulting from AEE of the films, acquired at $|\mu_0H|$ = 0.9 T. Here, ΔA represents $A_{+0.9\,T}-A_{0.0\,T}$ with $A_{+0.9\,T}$ and $A_{0.0\,T}$ respectively being the A values at μ_0H = +0.9 and 0.0 T and $\phi_{\Delta A}$ represents the lock-in phase of ΔA. In the inset graph, $\phi_{\Delta A}$ ≈200° signifies $A_{0.0\,T} > A_{+0.9\,T}$. During the AEE measurement, J_c = 60 mA, f = 25 Hz, and zero DC offset was applied to the sample. c) q dependence of $\Delta A/A$ for the as-deposited and 573 K-annealed $Co_{100-q}Cu_q$ composition-gradient films, simultaneously estimated using the proposed LIT-based GMR measurement technique. The black and red strips represent the q values exhibiting the largest $-\Delta A/A$ value for as-deposited and 573 K-annealed $Co_{100-q}Cu_q$ composition-gradient films, respectively. d) H dependence of R for the 573 K-annealed $Co_{100-q}Cu_q$ composition gradient film near the optimum composition ($Co_{22}Cu_{78}$) at 300 K. The maximum GMR ratio $\Delta R/R = (R_{+0.9\,T}-R_{0.0\,T})/R_{0.0\,T}$ for the optimum composition at room temperature was determined to be ≈8.1% for μ_0H = +0.9 T, which is consistent with the GMR ratio obtained by the LIT-based GMR measurement technique. $R_{+0.9\,T}$ and $R_{0.0\,T}$ represent the resistances at μ_0H = +0.9 and 0.0 T, respectively. e) H dependence of R at 4 K for the optimum composition. The saturation GMR ratio for the film was determined using the relation $\Delta R/R = (R_H-R_{max})/R_{max}$, where R_{max} and R_H represent the maximum and minimum resistances of the film near zero and at μ_0H = +5.0 T, respectively.

itates due to phase decomposition during the annealing treatment at 573 K, as reported in the literature.[60] While a detailed microstructural analysis of the films is beyond the scope of this work, the present study successfully demonstrates the effectiveness of the proposed LIT-based GMR measurement method for investigating composition-dependent GMR behaviors.

This high-throughput and systematic GMR measurement reveals that $Co_{22}Cu_{78}$ in the 573 K-annealed film exhibits a large GMR ratio ($-\Delta R/R \equiv -\Delta A/A$) of ≈8.8 ± 0.9% at μ_0H = +0.9 T and room temperature. This GMR ratio is the highest recorded among polycrystalline CoCu-based single-layer granular films of any composition.[42–45] Notably, a larger saturated GMR ratio of 20% has been reported for (111)-oriented epitaxial Co–Cu films in a previous study at room temperature.[54] However, in the same research, a much smaller saturated GMR ratio of 7% was observed at room temperature for (001)-oriented epitaxial Co–Cu films,[54] reflecting the high dependency of GMR on crystal orientation for epitaxial Co–Cu films. We note that the previous study defined the saturated GMR ratio differently, using the maximum change in R over the measurement H range divided by the R at high H. Following the same approach for our current film yields a GMR ratio of ≈9.6 ± 0.8% at μ_0H = +0.9 T and room temperature. While larger GMR ratios can be achieved in epitaxial films on single-crystalline substrates, their use in commercial applications is limited due to the complexity of film fabrication and the high cost of single-crystalline substrates. Therefore, the observation of a large GMR ratio in polycrystalline CoCu-based single-layer granular films at room temperature is crucial.

To confirm the best GMR value obtained from the LIT-based high-throughput screening, we conducted conventional four-probe GMR measurements for the same film near the optimal composition region. For the measurement, we used the 573 K-annealed $Co_{100-q}Cu_q$ composition-gradient film patterned into parallel wire shapes perpendicular to the direction of the composition gradient. Each wire had a width of 0.4 mm and a spacing of 0.4 mm. It is important to note that we can neglect the compositional variation along the width direction for these wires, which is ≈2.0%. Figure 5d shows the H dependence of R for the wire near the optimum composition of $Co_{22}Cu_{78}$ recorded at 300 K. Utilizing the relation $\Delta R/R = (R_{+0.9\,T}-R_{0.0\,T})/R_{0.0\,T}$, where $R_{+0.9\,T}$ and $R_{0.0\,T}$ respectively represent the resistances at μ_0H = +0.9 and 0.0 T, we determined the GMR ratio for the film composition to

be 8.1% which is consistent with the results obtained from the LIT-based measurements. In Figure 5e, we present the H dependence of R for the same film at 4 K. The data reflect the saturation behavior of the R of the film with minimum R at high H and a maximum R at finite $\pm H$, which can be correlated with the coercivity field of the film.[6] Since the maximum R occurs at finite $\pm H$, not at zero, we use $(R_H - R_{max})/R_{max}$ instead of $(R_H - R_0)/R_0$ to determine the saturation GMR ratio for the film at 4 K, where R_{max} and R_H represent the maximum and minimum resistance values of the film, respectively (Figure 5e). The saturation GMR ratio obtained using the above relation was observed to be 28.0%. In comparison, for a previously reported $Co_{20}Cu_{80}$ single-layer granular film, fabricated by magnetron sputtering onto a quartz glass substrate, a maximum GMR ratio of 16.5% was achieved at 5 K at $\mu_0 H = 5.0$ T.[6]

This demonstration clearly illustrates the effectiveness of the LIT-based GMR measurement method in accelerating the optimization of materials and devices, presenting clear advantages over traditional GMR measurements. This method eliminates the need to fabricate many films or numerous Hall bars, which are often required for conventional GMR measurements, making the process time-consuming and laborious. Furthermore, the LIT-based method utilizing composition-gradient and wedge-shaped films significantly enhances composition and thickness resolution, respectively, overcoming inherent limitations in conventional GMR measurement techniques that might lead to overlooking optimal compositions and layer thicknesses. Notably, for multilayers consisting of two-dimensional composition/thickness gradients, the method demonstrated here is effective for determining not only the optimum composition but also the optimal thickness of each layer. The utilization of the proposed LIT-based GMR measurement method with such two-dimensional multilayers to simultaneously assess multiple film parameters will further boost the optimization process of GMR materials and devices.

3. Conclusion

We proposed and demonstrated a high-throughput screening method for assessing the GMR properties of materials by utilizing thermal imaging of Joule heating measured by the LIT technique. By utilizing the CoFe/Cu multilayer film, we confirmed the accurate and reliable estimation of the GMR ratio using this proposed method. Furthermore, the usefulness of this approach was demonstrated through its application to the composition-gradient CoCu-based magnetic granular films. The demonstration utilizing multiple composition-gradient films simultaneously highlighted the practicality of the proposed method for high-throughput optimization of film composition with precision. Furthermore, the high-throughput investigation revealed a previously unexplored CoCu-based granular composition with a GMR ratio exceeding 8% at $\mu_0 H = 0.9$ T at room temperature, and a saturation GMR ratio of ≈28% at 4 K, setting new record high values for polycrystalline CoCu-based single-layer granular materials. This advancement holds great promise for significantly improving the efficiency of material screening and design optimization processes for spintronics technology.

4. Experimental Section

Fabrication of CoFe/Cu Multilayer Film: The CoFe/Cu multilayer film used in this study possessed the following structure: $Co_{50}Fe_{50}$(3.0 nm)/[Cu(1.6 nm)/$Co_{50}Fe_{50}$(3.0 nm)]$_{33}$, where the numbers in the parentheses denote the thicknesses of the layers and the subscript 33 denotes the number of the repeated depositions. This film was deposited on a single-crystalline MgO (001) substrate at room temperature using magnetron sputtering. A 5 nm-thick Al layer was deposited on the multilayer without breaking the vacuum to prevent sample oxidation. The as-deposited film was post-annealed at 523 K in a vacuum while applying an in-plane magnetic field of 0.3 T for 1 h. This film is identical to that utilized in the previous study,[46] where comprehensive details regarding its fabrication conditions are available.

Fabrication of $Co_{100-q}Cu_q$ Composition-Gradient Granular Film: The $Co_{100-q}Cu_q$ composition-gradient films with a thickness of 100 nm were fabricated on 10 × 10 mm^2 quartz glass substrates using a magnetron sputtering system (Comet, Inc., CMS-3200). Before deposition, the chamber was evacuated at a base pressure of $< 6.0 \times 10^{-6}$ Pa using a cryopump. Then, the films were deposited at a process Ar gas pressure of 0.4 Pa at ambient temperature using DC power sources. The previously established layer-by-layer wedge-shaped deposition process was followed to achieve a composition variation of $65 \leqslant q \leqslant 100$ at.% over a length of 7.0 mm on a single substrate.[57–59] This process involved three consecutive steps: I) initial deposition of a uniform Cu layer, followed by the deposition of a wedge-shaped Cu layer using a linear moving shutter over a length of 7.0 mm, II) 180° rotation of the substrate, and III) subsequent deposition of a wedge-shaped Co layer. After completing the steps (I)–(III), the total thickness was designed to be 0.5 nm. This sequence was repeated 200 times to obtain the 100 nm-thick composition-gradient film. The deposition rates of the Cu and Co layers were maintained at 0.023 and 0.025 nms^{-1}, respectively. The deposition duration at each step was optimized to obtain the desired composition. A 2 nm-thick Al layer was applied as a cap to prevent oxidation. One of the room-temperature-deposited films was annealed at 573 K for 10 min in a vacuum atmosphere to boost the formation of the granular structure.

Acknowledgements

This work was supported by ERATO "Magnetic Thermal Management Materials" (grant no. JPMJER2201) from JST, Japan, the Grant-in-Aid for Scientific Research (S) (grant no. 22H04965), and the Grant-in-Aid for Early-Career Scientists (grant no. 21K14519) from JSPS KAKENHI, Japan, and NEC Corporation. R.M. was supported by JSPS through the "JSPS Postdoctoral Fellowship for Research in Japan (Standard)" (grant no. P21064).

Conflict of Interest

The authors declare no conflict of interest.

Data Availability Statement

The data that support the findings of this study are available from the corresponding author upon reasonable request.

Keywords

combinatorial deposition, giant magnetoresistance effect, granular films, high-throughput material screening, lock-in thermography

Received: February 14, 2024
Revised: April 21, 2024
Published online: May 24, 2024

[1] M. N. Baibich, J. M. Broto, A. Fert, F. N. Van Dau, F. Petroff, P. Etienne, G. Creuzet, A. Friederich, J. Chazelas, *Phys. Rev. Lett.* **1988**, *61*, 2472.
[2] G. Binasch, P. Grünberg, F. Saurenbach, W. Zinn, *Phys. Rev. B* **1989**, *39*, 4828.
[3] S. S. P. Parkin, N. More, K. P. Roche, *Phys. Rev. Lett.* **1990**, *64*, 2304.
[4] S. S. P. Parkin, *Appl. Phys. Lett.* **1992**, *61*, 1358.
[5] A. E. Berkowitz, J. R. Mitchell, M. J. Carey, A. P. Young, S. Zhang, F. E. Spada, F. T. Parker, A. Hutten, G. Thomas, *Phys. Rev. Lett.* **1992**, *68*, 3745.
[6] J. Q. Xiao, J. S. Jiang, C. L. Chien, *Phys. Rev. Lett.* **1992**, *68*, 3749.
[7] K. B. Fathoni, Y. Sakuraba, Y. Miura, T. Sasaki, T. Nakatani, K. Hono, *J. Phys. D. Appl. Phys.* **2022**, *55*, 125001.
[8] K.-M. Lenssen, H. van Kesteren, T. G. S. Rijks, J. C. Kools, M. de Nooijer, R. Coehoorn, W. Folkerts, *Sensors Actuators A Phys* **1997**, *60*, 90.
[9] K. Kapser, M. Weinberger, W. Granig, P. Slama, *Smart Sensors, Measurement and Instrumentation*, Springer International Publishing, New York City **2013**, 133.
[10] J. C. Rife, M. M. Miller, P. E. Sheehan, C. R. Tamanaha, M. Tondra, L. J. Whitman, *Sensors Actuators A Phys* **2003**, *107*, 209.
[11] S. Ota, A. Ando, D. Chiba, *Nat. Electron.* **2018**, *1*, 124.
[12] S. Yamada, K. Chomsuwan, M. Iwahara, *5th IEEE Conference on Sensors*, IEEE, Daegu, Korea (South), **2006**, 927.
[13] M. Ha, G. S. Cañón Bermúdez, J. A.-C. Liu, E. S. Oliveros Mata, B. A. Evans, J. B. Tracy, D. Makarov, *Adv. Mater.* **2021**, *33*, 2008751.
[14] P. D. Kulkarni, H. Iwasaki, T. Nakatani, *Sensors* **2022**, *22*, 9385.
[15] K. Wu, D. Tonini, S. Liang, R. Saha, V. K. Chugh, J.-P. Wang, *ACS Appl. Mater. Interfaces* **2022**, *14*, 9945.
[16] S. Liang, P. Sutham, K. Wu, K. Mallikarjunan, J.-P. Wang, *Sensors* **2022**, *22*, 5663.
[17] Y. Dong, T. Xu, W. Jiang, *Appl. Phys. Lett.* **2021**, *119*, 192403.
[18] M. Ha, G. S. Cañón Bermúdez, T. Kosub, I. Mönch, Y. Zabila, E. S. Oliveros Mata, R. Illing, Y. Wang, J. Fassbender, D. Makarov, *Adv. Mater.* **2021**, *33*, 2005521.
[19] D. Su, K. Wu, K. Srinivasan, Z. Nemati, R. Zamani, V. Chugh, R. Saha, R. Franklin, J. Modiano, B. Stadler, J. Wang, *Adv. Mater. Interfaces* **2023**, *10*, 2201417.
[20] T. Miyazaki, N. Tezuka, *J. Magn. Magn. Mater.* **1995**, *139*, L231.
[21] J. S. Moodera, L. R. Kinder, T. M. Wong, R. Meservey, *Phys. Rev. Lett.* **1995**, *74*, 3273.
[22] S. Yuasa, T. Nagahama, A. Fukushima, Y. Suzuki, K. Ando, *Nat. Mater.* **2004**, *3*, 868.
[23] S. S. P. Parkin, C. Kaiser, A. Panchula, P. M. Rice, B. Hughes, M. Samant, S.-H. Yang, *Nat. Mater.* **2004**, *3*, 862.
[24] T. Scheike, Z. Wen, H. Sukegawa, S. Mitani, *Appl. Phys. Lett.* **2023**, *122*, 112404.
[25] L. Piraux, J. M. George, J. F. Despres, C. Leroy, E. Ferain, R. Legras, K. Ounadjela, A. Fert, *Appl. Phys. Lett.* **1994**, *65*, 2484.
[26] A. Vedyayev, M. Chshiev, N. Ryzhanova, B. Dieny, C. Cowache, F. Brouers, *J. Magn. Magn. Mater.* **1997**, *172*, 53.
[27] H. Yuasa, M. Yoshikawa, Y. Kamiguchi, K. Koi, H. Iwasaki, M. Takagishi, M. Sahashi, *J. Appl. Phys.* **2002**, *92*, 2646.
[28] R. Saeki, S. Mizoguchi, H. Kamimura, M. Hayashida, T. Ohgai, *J. Magn. Magn. Mater.* **2021**, *529*, 167849.
[29] B. Dieny, P. Humbert, V. S. Speriosu, S. Metin, B. A. Gurney, P. Baumgart, H. Lefakis, *Phys. Rev. B* **1992**, *45*, 806.
[30] M. Xu, Y. Fan, G. Luo, Z. Mai, *Phys. Lett. A* **2000**, *272*, 282.
[31] D. Meziane Mtalsi, M. El Harfaoui, A. Qachaou, M. Faris, J. Ben Youssef, H. Le Gall, *Phys. status solidi* **2001**, *187*, 633.
[32] I. Bakonyi, E. Simon, B. G. Tóth, L. Péter, L. F. Kiss, *Phys. Rev. B* **2009**, *79*, 174421.
[33] M. Suzuki, Y. Taga, A. Goto, H. Yasuoka, *J. Magn. Magn. Mater.* **1993**, *126*, 495.
[34] W. Kuch, A. C. Marley, S. S. P. Parkin, *J. Appl. Phys.* **1998**, *83*, 4709.
[35] P. D. Kulkarni, T. Nakatani, Z. Li, T. Sasaki, Y. Sakuraba, *J. Magn. Magn. Mater.* **2022**, *560*, 169562.
[36] K. B. Fathoni, Y. Sakuraba, T. Sasaki, Y. Miura, J. W. Jung, T. Nakatani, K. Hono, *APL Mater.* **2019**, *7*, 111106.
[37] D. Taparia, K. B. Fathoni, P. D. Kulkarni, A. Srinivasan, P. Alagarsamy, Y. Sakuraba, T. Nakatani, K. Hono, *J. Magn. Magn. Mater.* **2021**, *538*, 168321.
[38] O. Breitenstein, W. Warta, M. Langenkamp, *Lock-In Thermography: Basics and Use for Evaluating Electronic Devices and Materials*, Springer Berlin Heidelberg, Berlin, Heidelberg **2010**, *10*.
[39] S. Daimon, R. Iguchi, T. Hioki, E. Saitoh, K. Uchida, *Nat. Commun.* **2016**, *7*, 13754.
[40] S. Daimon, K. Uchida, R. Iguchi, T. Hioki, E. Saitoh, *Phys. Rev. B* **2017**, *96*, 024424.
[41] K. Uchida, S. Daimon, R. Iguchi, E. Saitoh, *Nature* **2018**, *558*, 95.
[42] A. N. Pohorilyi, A. F. Kravetz, E. V. Shipil, A. Y. Vovk, C. S. Kim, H. R. Khan, *J. Magn. Magn. Mater.* **1998**, *186*, 87.
[43] G. Wen, H. Zhao, J. Zhao, X. Zhang, *Mater. Sci. Eng. C* **2001**, *16*, 81.
[44] I. O. Shpetnyi, D. M. Kondrakhova, S. I. Vorobiov, B. Scheibe, V. I. Grebinaha, D. O. Derecha, Y. I. Gorobets, I. Y. Protsenko, *J. Magn. Magn. Mater.* **2019**, *474*, 624.
[45] Z. Yan, B. Wang, X. W. Lv, W. B. Sui, J. W. Cao, H. G. Shi, M. S. Si, D. Z. Yang, D. S. Xue, *Appl. Phys. Lett.* **2020**, *116*, 42401.
[46] T. Hirai, Y. Sakuraba, K. Uchida, *Appl. Phys. Lett.* **2022**, *121*, 162404.
[47] H. Straube, O. Breitenstein, *J. Appl. Phys.* **2011**, *109*, 064515.
[48] T. Seki, R. Iguchi, K. Takanashi, K. Uchida, *Appl. Phys. Lett.* **2018**, *112*, 152403.
[49] T. Seki, R. Iguchi, K. Takanashi, K. Uchida, *J. Phys. D. Appl. Phys.* **2018**, *51*, 254001.
[50] T. Seki, A. Miura, K. Uchida, T. Kubota, K. Takanashi, *Appl. Phys. Express* **2019**, *12*, 023006.
[51] R. Das, R. Iguchi, K. Uchida, *Phys. Rev. Appl.* **2019**, *11*, 034022.
[52] R. Modak, K. Uchida, *Appl. Phys. Lett.* **2020**, *116*, 032403.
[53] J. Q. Xiao, J. S. Jiang, C. L. Chien, *Phys. Rev. B* **1992**, *46*, 9266.
[54] S. S. P. Parkin, R. F. C. Farrow, T. A. Rabedeau, R. F. Marks, G. R. Harp, Q. Lam, C. Chappert, M. F. Toney, R. Savoy, R. Geiss, *Europhys. Lett.* **1993**, *22*, 455.
[55] K. Miyazaki, S. Kainuma, K. Hisatake, T. Watanabe, N. Fukumuro, *Electrochim. Acta* **1999**, *44*, 3713.
[56] V. V. Hiep, N. Chau, D. M. Hong, N. H. Luong, *J. Magn. Magn. Mater.* **2007**, *310*, 2524.
[57] H. Masuda, R. Modak, T. Seki, K. Uchida, Y.-C. Lau, Y. Sakuraba, R. Iguchi, K. Takanashi, *Commun. Mater.* **2020**, *1*, 75.
[58] R. Modak, K. Goto, S. Ueda, Y. Miura, K. Uchida, Y. Sakuraba, *APL Mater.* **2021**, *9*, 031105.
[59] R. Modak, Y. Sakuraba, T. Hirai, T. Yagi, H. Sepehri-Amin, W. Zhou, H. Masuda, T. Seki, K. Takanashi, T. Ohkubo, K. Uchida, *Sci. Technol. Adv. Mater.* **2022**, *23*, 767.
[60] T. Sugawara, K. Takanashi, H. Fujimori, *J. Magn. Magn. Mater.* **1998**, *177–181*, 951.